ACS OMEGA

http://pubs.acs.org/journal/acsodf

Article

Grafting Polymerization of Long-Chain Hydrophobic Acrylic Monomer onto Lignin and Its Application in Poly(Lactic Acid)-Based Wholly Green UV Barrier Composite Films

Kang Shi, Guoshuai Liu, Hui Sun,* Biao Yang, and Yunxuan Weng*

Cite This: *ACS Omega* 2023, 8, 26926−26937

Read Online

ACCESS | Metrics & More | Article Recommendations | Supporting Information

ABSTRACT: The development of low-cost and high-performance bio-based composites derived from forestry waste lignin and polylactic acid has emerged as a topic of central attention. However, the weak compatibility between lignin and polylactic acid often resulted in high brittleness of the composites. Graft copolymerization is not only the most effective way to modify lignin but also can significantly improve the compatibility of lignin and polylactic acid. In this study, bio-based monomer lauryl methacrylate was grafted onto lignin by feasible radical polymerization to prepare lignin graft copolymers with excellent thermal stability and hydrophobicity, which are expected to improve the compatibility with polylactic acid. Wholly bio-based composites were prepared by compounding this graft copolymer with polylactic acid. The results showed that the crystallization ability of the composite was improved, and the highest crystallinity was increased from 6.42% to 17.46%. With addition of LG-g-PLMA lower than 9%, the thermal stability of the composites was slightly improved. At 5% copolymer addition, the elongation at break and tensile toughness of the composites increased by 42% and 36%, respectively. Observation of the frozen fracture surface of the composite by SEM found that wire drawing and ductile deformation appeared when a small amount of LG-g-PLMA was added. The thus prepared composites also showed excellent UV barrier properties. This approach provides a new idea for the high-value application of lignin.

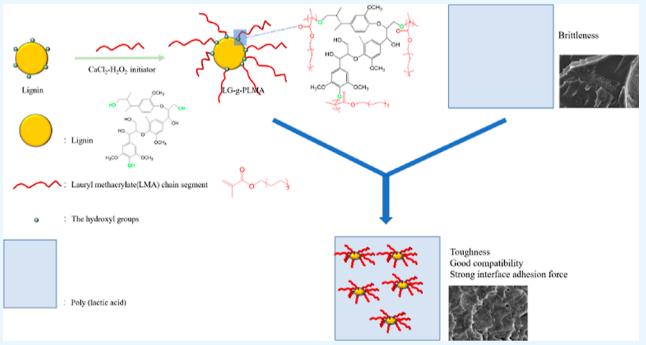

1. INTRODUCTION

At a time when oil resources are increasingly scarce and environmental pollution is becoming more and more serious, the use of renewable materials and materials in line with sustainable development has become necessary. Therefore, the development and application of bio-based polymer materials which can replace traditional petroleum-based materials[1,2] has been receiving much research attention. In this regard, polylactic acid (PLA) is considered to be the most promising biomaterial because of its excellent reproducibility, degradability, and wide availability from renewable resources.[3] In addition to its biodegradable properties, PLA also has outstanding mechanical and physical properties, such as high strength, transparency, easy processing, and so on. The tensile strength can reach 50−70 MPa.[4] PLA can be processed conveniently by injection molding, film blow molding, and other commercial methods in a temperature range of 170−230 °C.[5] Therefore, PLA is widely used in many fields, such as 3D printing,[6,7] food packaging,[8,9] biomedical field,[10,11] adhesives,[12,13] and so forth. However, the rigidity of the main chain structure of PLA determines the brittleness[14] and low elongation at break (4−6%),[15] which limits its application in a wide range of fields.

In recent years, extensive efforts have been made to the toughening of PLA. For example, petroleum-based derivatives such as polyethylene or chain extenders[16−18] were compounded with PLA for the purpose of reducing the brittleness. However, the addition of these non-degradable toughing agents inevitably deteriorates the degradability of PLA. In contrast, the use of biopolymers has no adverse effect on biodegradability of PLA composites and helps overcome the brittleness of PLA. Lignin, as a very abundant biomass resource after cellulose, is also the only biopolymer containing a benzene ring among plant resources. Advantages of this polymer include low cost, abundant reserves, and excellent antioxidation and UV resistance. When applied to PLA, lignin is expected not only to increase its value-added utilization, but also play a role in the development of wholly green composites.[19]

Received: March 15, 2023
Accepted: July 14, 2023
Published: July 23, 2023

https://doi.org/10.1021/acsomega.3c01738
ACS Omega 2023, 8, 26926−26937

Lignin has an amorphous structure, with a 3D network composed of *p*-hydroxyphenyl alcohol (H), guaiacyl (G), and syringyl (S) through carbon−carbon and ether bonds.[20,21] Lignin contains a large number of active functional groups, such as methoxy, phenolic hydroxyl, alcohol hydroxyl, carbonyl, etc., which are available for direct functionalization. However, the presence of a large number of hydroxyls lead to the formation of hydrogen bonds and the benzene ring structure causes $\pi-\pi$ stacking. Because lignin is immiscible with PLA, the composites often have unsatisfactory mechanical properties.[22] In light of this issue, modifications of lignin by chemical modification are necessary.

Studies showed that direct modification of lignin via esterification[23,24] and hydroxymethylation[25] can only enhance the compatibility between lignin and PLA and elevate the mechanical properties of the composites to a limited extent. Modification strategies for better compatibility and comprehensive composite performance remain a challenge. Graft copolymerization has been reported as one of the most effective ways to realize the high-value utilization of lignin. By introducing functional monomers into lignin, the compatibility between PLA and lignin can be significantly improved. In addition, the grafting monomers also render lignin desirable functions.[26]

Free-radical polymerization,[27,28] ring-opening polymerization,[29,30] and living radical polymerization[31,32] have been reported for the preparation of graft copolymers. Among them, free-radical polymerization is the simplest and most effective method. Examples of the advantages are its applicability to a wide range of monomers (including acrylic acid[33] and styrene[34]) and various polymerization methods that are easy to operate and of low cost. This method has been widely used in grafting of many monomers onto lignin.[35]

These grafted copolymers exhibit some impressive properties, such as heat resistance, hydrophobicity, and UV resistance, and can be used in a wide range of applications.[36,37] The incorporation of these copolymers to PLA can bring some unique properties to the composites and enrich their applications.

In this study, we improved the free-radical polymerization methods commonly used in lignin modification. By our modified procedure, the grafting reaction time was greatly shortened from 12 or 24 to 6 h, and the grafting efficiency was improved. The selected $CaCl_2-H_2O_2$ initiator system was not only very efficient but also highly selective for grafting acrylic monomer onto lignin,[28,36] with the initiating efficiency of more than 90% and almost no homopolymer formation.

Lignin copolymers were prepared by grafting lauryl methacrylate (LMA), a renewable fatty acid synthesized from plant oil, onto lignin by free-radical polymerization.[27,32,38,39] Thermal properties, hydrophobicity, and chemical structure before and after grafting polymerization were investigated. With a long hydrophobic side chain, LMA monomer is expected to improve the hydrophobicity and flexibility of lignin. The addition of the copolymer is expected to significantly improve the compatibility of lignin with PLA, thus overcoming the brittleness. In addition, the introduction of lignin would also impart UV barrier properties to PLA. This approach provides an idea for the application of wholly green packaging materials in the field of UV barriers.

2. MATERIALS AND METHODS

2.1. Materials. Poly(lactic acid) (PLA, 4032D) was purchased from Nature Works LLC. Lignin was purchased from Shandong Longlive Biotechnology Co., Ltd., China. Lauryl methacrylate (LMA) (stabilized, 96%) was obtained from Macklin Chemical Reagent Co., Ltd., China. Dimethyl sulfoxide (DMSO, AR), hydrogen peroxide (H_2O_2, AR), hydrochloric acid (HCl), and calcium chloride (NaCl, AR) were supplied by Fuchen Chemical Reagent Co., Ltd., China.

2.2. Experimental Method. *2.2.1. Synthesis of Lignin-Graft-Poly(Lauryl Methacrylate) (LG-g-PLMA).* Under a nitrogen atmosphere, 1.0 g of calcium chloride and 20 mL of DMSO were added to a flask and stirred until calcium chloride was completely dissolved. Then, 1.0 g of lignin was added and the reaction was heated up to 50 °C, stirred for 30 min until complete dissolution of lignin. Finally, 4.0 g of LMA and 1 mL of hydrogen peroxide were added to the flask and the reactants were stirred for 6 h.

At the end of the reaction, the solution was added dropwise into dilute hydrochloric acid of pH = 3 to precipitate. The precipitate was filtered out and washed with deionized water. Then, the final product LG-g-PLMA was obtained by vacuum drying. The graft efficiency of the copolymer was calculated to be 76.8% using eq 1.[27,28,36]

$$G(\%) = \frac{W_2 - W_1}{W_0} \times 100\% \quad (1)$$

where W_2 is the weight of the grafting copolymer, W_1 is the weight of LG used, and W_0 stands for the weight of monomers used in the experiments.

2.2.2. Preparation of the PLLA/LG-g-PLMA Composite. PLA was dried at 80 °C for 8 h in a vacuum drying oven. LG-g-PLMA was dried at 60 °C for 24 h in a vacuum drying oven. Afterward, the dried PLA and LG-g-PLMA of various proportions (Table 1) were added to a micro twin-screw extruder and were mixed at 185 °C for 7 min at a speed of 60 rpm to form the PLLA/LG-g-PLMA composite. Control sample PLA/5% lignin was also prepared according to the same procedure for comparison.

Table 1. Composition of PLLA/LG-g-PLMA Composites

sample	PLA (wt %)	LG-g-PLMA (wt %)	LG (wt %)
PLLA	100	0	0
PLLA1	99	1	0
PLLA2	97	3	0
PLLA3	95	5	0
PLLA4	93	7	0
PLLA5	91	9	0
PLLA6	80	20	0
PLLA7	95	0	5

Then, a certain amount of the composite was placed in a mold (80 mm long and wide, 0.4 mm thick) and hot-pressed for 5 min at 190 °C to obtain a thin slice for further test.

2.3. Characterization. *2.3.1. Differential Scanning Calorimetry.* Differential scanning calorimetry (DSC, Q100, TA, USA) was used to investigate the non-isothermal crystallization of the composites. Samples were equilibrated at 200 °C for 3 min to erase the thermal history. Then, they were cooled to 30 °C at 10 °C/min. Finally, the samples were reheated from 30 to 200 °C at the same rate. The degree of

https://doi.org/10.1021/acsomega.3c01738
ACS Omega 2023, 8, 26926−26937

Scheme 1. Illustration of the Synthetic Route to LG-g-PLMA

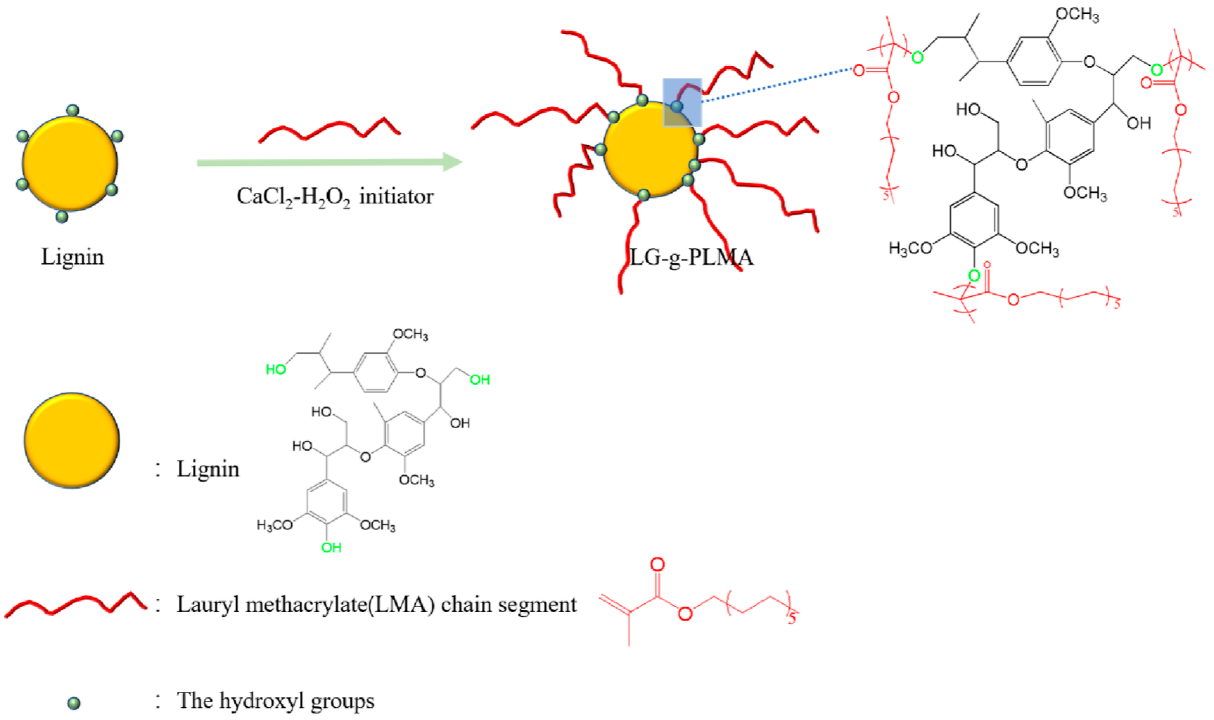

Scheme 2. Illustration of the Chemical Reaction in Synthesis of LG-g-PLMA

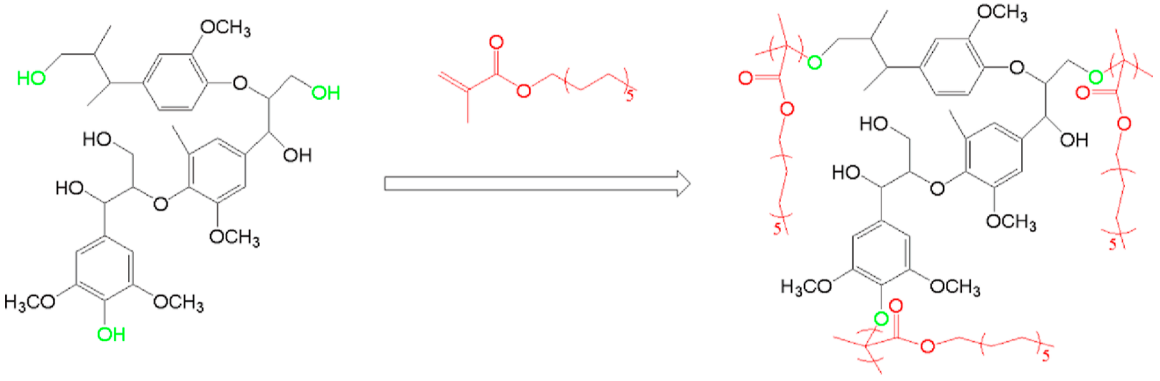

crystallinity (X_c) of composites was calculated according to eq 2

$$X_c = \frac{\Delta H_m}{(1 - \Phi_{\text{LG-g-PLMA}})\Delta H_{100\%\text{PLLA}}} \times 100\% \quad (2)$$

where ΔH_m is the melting enthalpy, $\Phi_{\text{LG-g-PLMA}}$ is the mass fraction of LG-g-PLMA, and $\Delta H_{100\%\text{PLLA}}$ is the melting enthalpy of pure PLLA ($\Delta H_{100\%\text{PLA}}$ = 93.7 J·g^{-1}).[40]

2.3.2. Scanning Electron Microscopy. The microscopic morphology of the cryo-fractured surfaces was observed by scanning electron microscopy (SEM, Thermo Quattro S) at 4000 times magnification. All specimens were sputter-coated with a thin layer of gold.

2.3.3. Mechanical Properties. All samples for the tensile test were prepared by cutting the thin slices. The tensile strength and elongation at break of the samples were tested by a microcomputer-controlled electronic universal testing machine (CMT6104, MTS Systems Co. Ltd., China) according to China national standard GB/T 1040.3-2006. Tensile specimens with 80 mm gauge length, 0.4 mm thickness, and 6 mm narrow section width were used at a rate of 5 mm/min. Five replicates were tested for each sample.

2.3.4. Fourier Transform Infrared Spectroscopy. Fourier transform infrared (FT-IR) spectra were recorded on a FT-IR spectrophotometer (iN10 MX) with wavenumbers in the range of 4000 to 400 cm^{-1}. Pellets of dried lignin or LG-g-PLMA were made with KBr. Each spectrum was collected with 32 scans and 2 cm^{-1} resolution at room temperature.

2.3.5. Thermogravimetric Analysis. Thermal stability of the composites was determined by using a thermogravimetric analyzer (STA7200 HITACHI). Experiments were performed in the temperature range from room temperature to 700 °C at a heating rate of 20 °C/min under a nitrogen atmosphere.

2.3.6. Rheological Properties. Rheological tests were carried out with a rotary rheometer (MARS, Thermo Scientific Co., Ltd.) at 190 °C. The angular velocity was set in the range of 0.01−100 rad/s.

2.3.7. Optical Property. The optical properties of pure PLLA and PLLA/LG-g-PLMA composites were characterized

https://doi.org/10.1021/acsomega.3c01738
ACS Omega 2023, 8, 26926−26937

on a UV−vis spectrophotometer (Shimadzu UV-3600-Plus, Japan) in the wavelength interval between 200 and 800 nm.

2.3.8. Gel Permeation Chromatography. Gel permeation chromatography (GPC) data of samples were obtained by a gel permeation chromatograph (Agilent infinity 1260-2). Monodispersed polystyrene (PS) was used as the standard, using THF as an eluent at a flow rate of 1.0 mL min^{-1} to generate the calibration curve.

2.3.9. Nuclear Magnetic Resonance. One-dimensional high-resolution ^1H NMR spectra were recorded at room temperature in deuterated chloroform (DMSO-d_6) using an NMR spectrometer (Bruker 600M).

2.3.10. Water Contact Angle. Water contact angles were obtained using a water contact angle measuring instrument (OCA35 DataPhysics Instruments GmbH). Lignin or LG-g-PLMA was dissolved in tetrahydrofuran and then was dripped onto a glass sheet through a rubber dropper and dried at 40 °C for 1 h for film formation. The obtained film was used for water contact angle measurements and the result was the average value of 5 times measurements.

3. RESULTS AND DISCUSSION

3.1. Structure Analysis of LG-g-PLMA. The synthesis of LG-g-PLMA is illustrated in Schemes 1 and 2. With the initiating system containing H_2O_2 and Cl^-, a concerted reaction may be occurring to form a hydroperoxide−chloride ion complex. The complex can extract hydrogen at the hydroxyl site of lignin to form lignin macromolecular free radicals. Macromolecular free radicals initiated the polymerization of LMA monomers and linked LMA molecules to lignin molecules.[27,28,41] Finally, these grafted chains were terminated by disproportionation, coupling, or chain transfer between living radicals or between radicals and macromolecules.[35]

A control reaction in the absence of lignin under the same experimental conditions was also carried out to confirm the key role of lignin in the grafting reaction. The results showed that no precipitation was observed after the addition of solution to dilute hydrochloric acid with no product residue after filtration, indicating that the grafting reaction was mainly carried out on lignin.

The FT-IR spectra of lignin before and after grafting are shown in Figure 1. Lignin has a broad absorption band observed near 3420 cm^{-1}, which is attributed to the stretching vibration of hydroxyl (−OH).The three stretching bands at 1600, 1513, and 1466 cm^{-1} in the pink region are derived from the characteristic absorption peaks of the lignin aromatic ring.[28] After the grafting reaction, a new characteristic absorption peak appeared at 1731 cm^{-1}, which was assigned to the −C═O group of LMA. At the same time, a new peak emerged at 1148 cm^{-1}, which was originated from to the C−O bond of the ester bond in LMA. These observations indicate the successful grafting of LMA on lignin.[27] In addition, the presence of a large number of $-CH_3$ and $-CH_2$ on the side chain of LMA significantly intensified the absorption peak at 2997 and 2951 cm^{-1}; In addition, a peak representing the $-CH_2$ group on the main chain of lauryl ester appeared at 750 cm^{-1}, further confirming the occurrence of the grafting polymerization.[39,42]

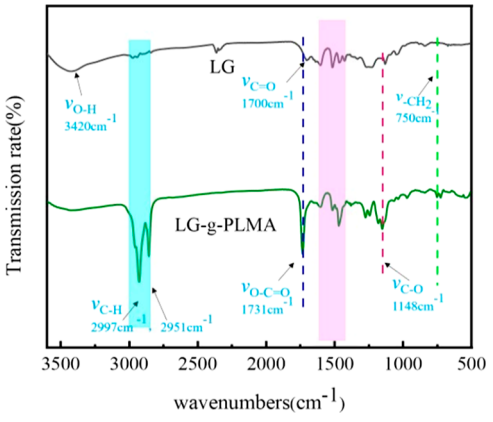

Figure 1. FT-IR spectra of lignin and LG-g-PLMA.

In addition to IR spectroscopy, both ^1H NMR and GPC were also applied to the characterization of the graft polymerization of lignin. It can be clearly seen from Figure 2

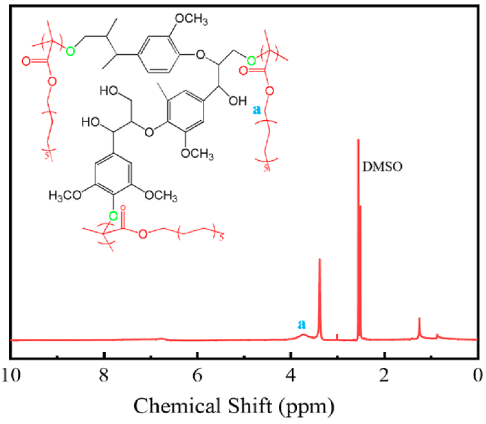

Figure 2. ^1H NMR spectrogram of LG-g-PLMA.

that a chemical shift occurs at δ = 3.74 ppm, which is the methylene proton peak of the adjacent ester bond in LG-g-PLMA, while the peak at δ = 1.24 ppm is attributed to the grafted dodecyl side chain of the methylene proton peak.

It was found from Figure 3 that LG-g-PLMA flowed out of the gel chromatographic column earlier than LG, indicating

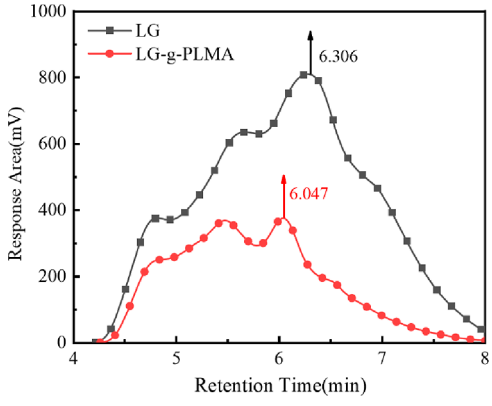

Figure 3. GPC curves of LG and LG-g-PLMA.

that its molecular weight was larger than that of LG. This GPC characterization, together with IR and NMR results confirmed that LMA was successfully grafted onto lignin.

In order to verify the dissolution property difference of lignin before and after grafting polymerization, LG and LG-g-PLMA were dissolved and placed in glass bottles containing

https://doi.org/10.1021/acsomega.3c01738
ACS Omega 2023, 8, 26926−26937

quantitative chloroform (2 mg/mL) and pictures of their dissolution behavior were recorded. Figure 4 shows that after

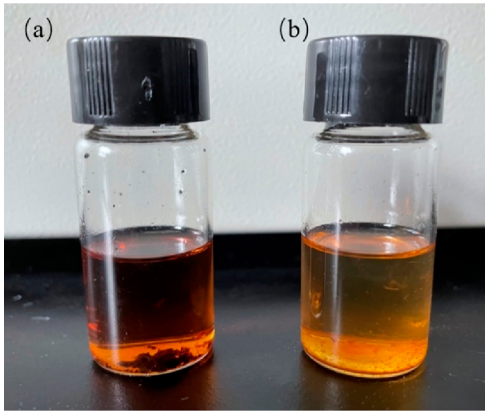

Figure 4. Solubilization characteristics of LG (a) and LG-g-PLMA (b) in chloroform for 24 h.

standing for 24 h, obvious precipitation appeared in LG bottle, with overall dark solution color. In comparison, LG-g-PLMA is almost completely dispersed in chloroform and has a lighter color. Because of the excellent solubility of LMA in chloroform, it is beneficial to the dissolution and dispersion of LG-g-PLMA in chloroform. The improved solubility of LG-g-PLMA in chloroform verified the success of the grafting reaction.

3.2. Thermal Stability of LG and LG-g-PLMA. The thermal stability of LG and LG-g-PLMA was characterized by thermogravimetric analysis (TGA). The TGA and DTG curves are displayed in Figure 5a,b respectively. Thermal decomposition data of LG and LG-g-PLMA are summarized in Table 2. It was found that LG began to decompose at 198.3 °C ($T_{5\%}$), with the highest decomposition rate at 346.1 °C (T_{max}). LG-g-PLMA began to decompose at 242.5 °C, which is 44.2 °C higher than that of LG, and the decomposition rate reached the maximum at 397.4 °C. This means that the lignin main chain was successfully grafted with LMA, thus improving the thermal stability.[43,44] It was also found that the residual amount of LG (40.6%) at high temperatures is much higher than that of LG-g-PLMA (13.3%). This is because LG contains

Table 2. Thermal Property Parameters of LG and LG-g-PLMA

sample	$T_{5\%}$ (°C)	T_{max} (°C)	residues at 700°C (%)
LG	198.3	346.1	40.6
LG-g-PLMA	242.5	397.4	13.3

a large number of aromatic rings and is more likely to form coke at high temperature, which is not easy to decompose.[45]

3.3. Water Contact Angle. The hydrophobicity of LG and LG-g-PLMA films was measured by a contact angle measuring instrument. The test sample is prepared by dissolving a small amount of powder in tetrahydrofuran. Then, the solution was dropped on a glass slide through an eyedropper. Figure 6

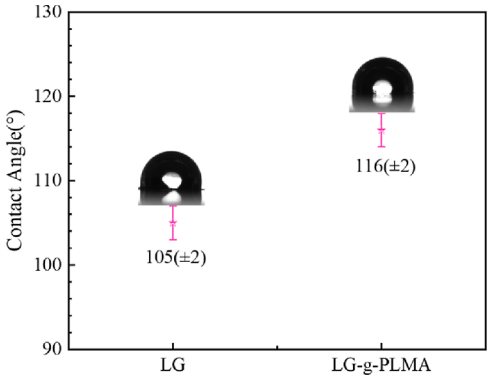

Figure 6. Water contact angles of LG and LG-g-PLMA.

shows that LG has a contact angle of 105°, indicating that the LG powder is hydrophobic. After the introduction of LMA, the contact angle is further increased to 116°, indicating that the hydrophobicity has been improved. The emergence of this phenomenon is mainly affected in two aspects. On the one hand, LMA molecule has a hydrophobic long chain containing 12C atoms. After grafting, these hydrophobic long-chain alkanes cover the surface of LG.[28] On the other hand, after the introduction of LMA, the effective number of hydroxyl groups of LG molecules is reduced, thus the hydrophobicity is improved. The widened absorption peak of hydroxyl groups at 3420 cm^{-1} in Figure 1 well illustrates this phenomenon.

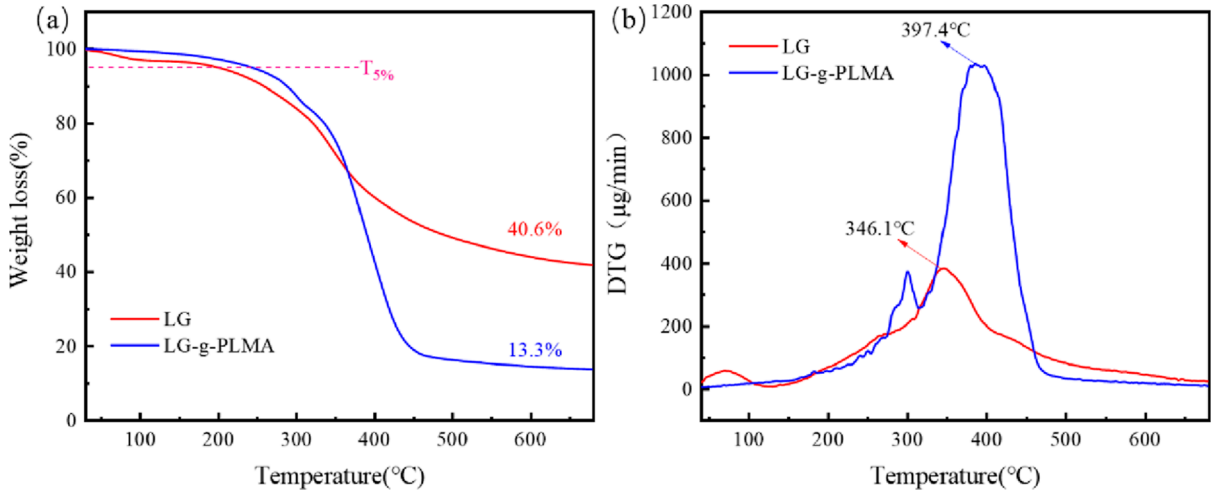

Figure 5. TGA curves (a) and DTG curves (b) of LG and LG-g-PLMA.

https://doi.org/10.1021/acsomega.3c01738
ACS Omega 2023, 8, 26926−26937

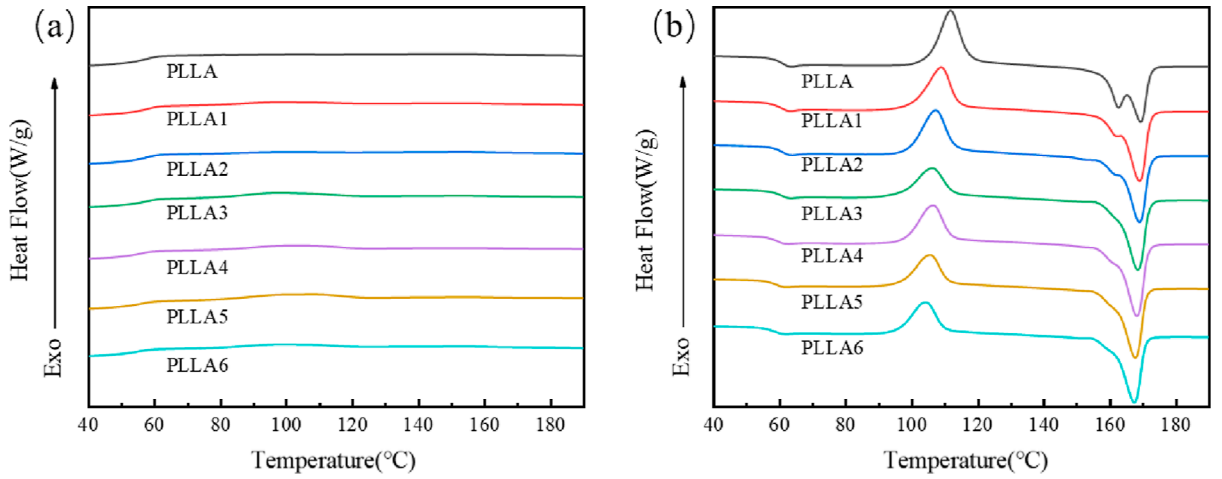

Figure 7. DSC curves of PLLA/LG-g-PLMA for cooling (a) and reheating (b) processes under the same rate of 10 °C/min.

Table 3. Non-isothermal Crystallization Parameters of PLLA and PLLA/LG-g-PLMA Composites

sample	T_g (°C)	T_{cc} (°C)	T_m (°C)	ΔH_{cc} (J/g)	ΔH_m (J/g)	X_c (%)
PLLA	61.53	111.80	158.39/169.35	30.95	36.97	6.42
PLLA1	61.35	109.20	162.82/169.15	27.05	39.26	13.16
PLLA2	61.22	107.21	163.00/169.04	27.16	36.38	10.58
PLLA3	60.60	106.03	162.27/168.56	20.12	34.71	16.38
PLLA4	59.46	106.39	162.29/168.28	23.19	35.44	14.06
PLLA5	59.21	105.38	161.68/167.78	19.57	34.44	17.44
PLLA6	58.66	104.00	161.38/167.58	19.03	32.12	17.46

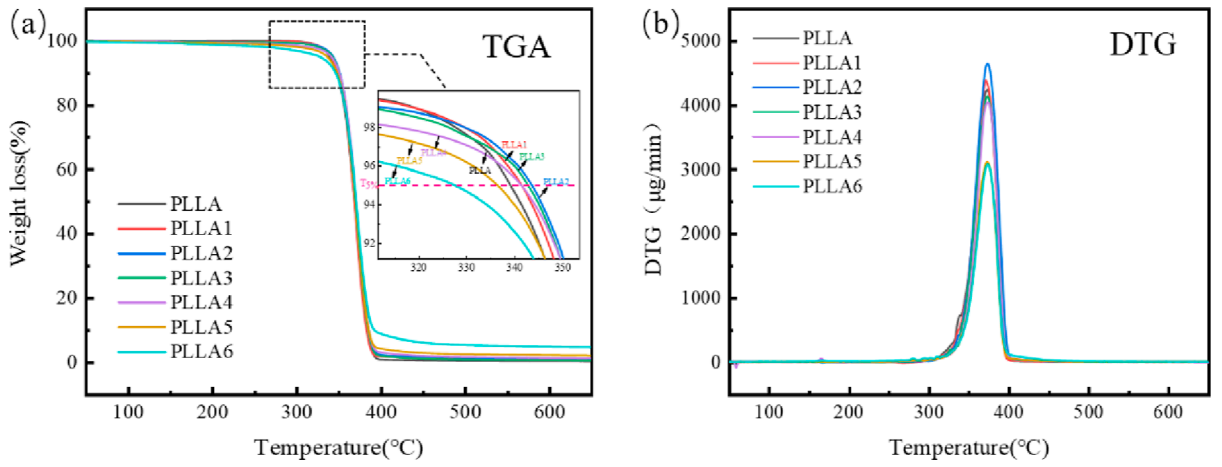

Figure 8. TGA (a) and DTG (b) curves of PLLA/LG-g-PLMA composites.

3.4. Thermal Properties of PLLA/LG-g-PLMA Composites. The effect of LG-g-PLMA on non-isothermal crystallization and melting crystallization of PLA was studied by DSC. It can be seen from Figure 7 and Table 3 that no crystallization peak was observed in the cooling stage. In the heating stage, PLA has a large cold crystallization peak, with T_{cc} of around 111.8 °C, and a crystallinity of 6.42%, indicating a weak crystallization ability of PLA. This is because the rigidity of PLA molecular segments is so strong that it is difficult to arrange and stack them into ordered crystals. After the addition of LG-g-PLMA, the crystallization of PLA was promoted. With increasing LG-g-PLMA content, the crystallinity of the composites was increased up to 17.46%. With the addition of more than 5% LG-g-PLMA, in the cooling stage, the composite showed a weak crystallization peak around 90 °C. With the addition of LG-g-PLMA, T_{cc} decreased with increasing LG-g-PLMA loading; the crystallization became easier; and the crystallization ability of the composite was greatly improved. This is due to the nucleation effect of LG-g-PLMA addition, which increased the additional heterogeneous nucleation sites for the crystallization of PLA.[46] Double melting peaks were observed for pure PLA in the programed heating stage. The endothermic peak at the low-temperature side is corresponding to α' to α phase transition, while the peak at the high-temperature side is ascribed to the melting of α crystal.[47] It is obvious that with the increase of LG-g-PLMA, the low-temperature melting peak is less obvious. At an addition higher than 5%, the molten acromion at low temperature almost disappeared. This phenomenon shows that the crystallization degree of the composites becomes

https://doi.org/10.1021/acsomega.3c01738
ACS Omega 2023, 8, 26926−26937

perfect. It was also found that T_g of the composites decreased with the addition of the graft copolymer. Introducing the copolymer increases the fluidity of the PLA segment, and the chain segment can be better stacked into ordered crystals.

TGA results are displayed in Figure 8 and Table 4. It was found that the thermal stability of the composites is slightly improved after the introduction of LMA. Pure PLA began to decompose at 339.3 °C and decomposed quickly at approximately 373.5 °C. After low contents (1, 3, and 5%) of LG-g-PLMA was added, $T_{5\%}$ and T_{max} of PLLA/LG-g-PLMA composites were higher than those of PLA. Higher loading of LG-g-PLMA (7, 9, and 20%) resulted in a decrease in thermal stability of the composites, probably due to the uneven distribution of LG-g-PLMA in PLA. The addition of 5% unmodified lignin to PLA led to a sharp decrease of the thermal stability (Figure S4 and Table S3), with $T_{5\%}$ and T_{max} decreasing from 339.3 and 373.5 °C (pure PLA) to 311. and 359.9 °C, respectively. This phenomenon indicates a poor compatibility and the interfacial adhesion between PLA and lignin. In contrast, LG-g-PLMA greatly improved its compatibility with PLA. From Figure 8, it was found that the carbon residue of the composite was proportional to the addition amount of LG-g-PLMA (except 5% LG-g-PLMA). The presence of LG was responsible for the increase of the carbon-based residues of PLLA/LG-g-PLMA composites.[48]

Table 4. Thermal Property Parameters of PLLA and PLLA/LG-g-PLMA Composites

sample	$T_{5\%}$ (°C)	T_{max} (°C)	residues at 700°C (%)
PLLA	339.3	373.5	0.31
PLLA1	341.7	371.6	1.18
PLLA2	343.7	373.9	1.35
PLLA3	343.2	373.8	0.77
PLLA4	342.1	374.2	1.57
PLLA5	337.1	373.5	2.44
PLLA6	327.9	374.3	5.31

3.5. Rheological Properties of PLLA/LG-g-PLMA Composites. Rheological behavior can be used to characterize interfacial interaction between the polymer matrix and additives. Figure 9 shows the curves of storage modulus (G'), loss modulus (G''), complex viscosity (η^*), and loss factor (tan δ) of PLA and PLLA/LG-g-PLMA composites with respect to frequency (ω). It can be seen from Figure 9 that the G', G'', and η^* of the composites are lower than those of pure PLA. This was because the flexible segments of LG-g-PLMA weakened the winding between PLA chains. The movability of PLLA/LG-g-PLMA composites had been improved. Therefore, when subjected to external forces, the deformation

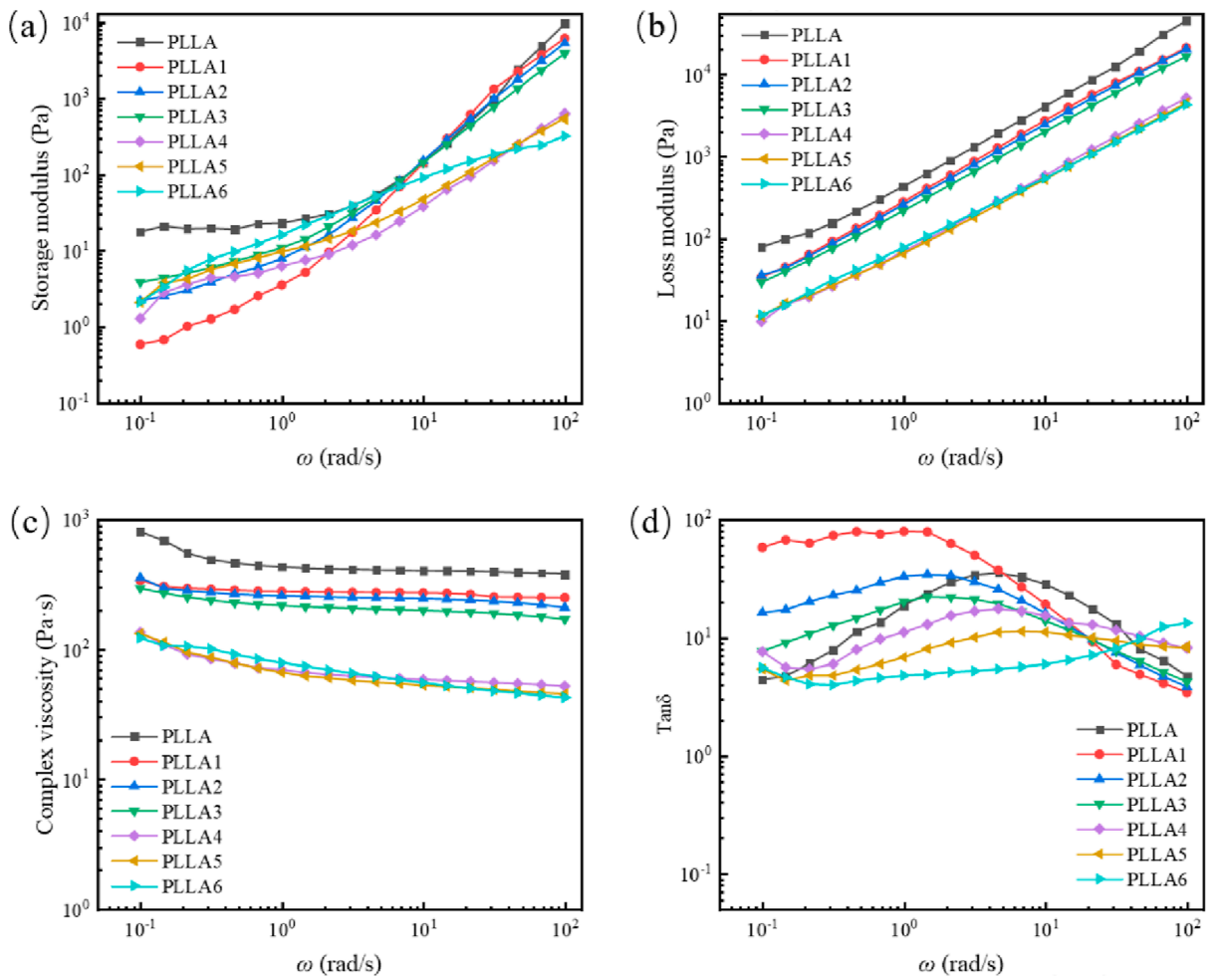

Figure 9. Frequency dependency of dynamic viscoelastic properties of PLLA and PLLA/LG-g-PLMA composites. (a) Storage modulus, (b) loss modulus, (c) complex viscosity, and (d) damping factor.

https://doi.org/10.1021/acsomega.3c01738
ACS Omega 2023, 8, 26926−26937

recovery between polymer chains becomes easier, resulting in the decrease of G''. It can be seen from Figure 9a that the G' in the low-frequency region increases with the increase of LG-g-PLMA addition, which is due to the entanglement of flexible segments in the polymer. LG-g-PLMA contains a large number of flexible segments of LMA, which increase the entanglement between molecular chains. Therefore, PLLA/LG-g-PLMA composites had higher G' on lower addition. With the continuous increase of frequency, the entanglement between the molecular chains is broken. The existence of LG-g-PLMA increases the free volume of the composite, and the chain segment moves more easily, thus exhibiting an opposite trend in comparison with the low-frequency region. The composite with higher LG-g-PLMA had a lower G'. A Newtonian platform as indicated by an obvious linear viscoelasticity was observed in Figure 9c. At the same time, the hydroxyl groups present on lignin easily cause chain fracture, leading to the decrease of viscosity of the composites.[32] The decreased η^* is, to some extent, conducive to reduce the energy consumption of the melt-processing of composites.[27] The addition of LG-g-PLMA reduced the viscosity of the composites, leading to obvious shear thinning in the low-frequency region. From Figure 9d, it can be seen that PLLA/LG-g-PLMA composites have higher tan δ than 1, indicating that $G'' > G'$, the melt viscosity behavior of the composite system is dominant. With more addition, the peak value of tan δ shifted to high frequency, indicating that the relaxation time of the molecular chain became shorter. This is because LG-g-PLMA segment hindered the winding between the PLA polymer chains, which enhanced the mobility of the molecular chain.

3.6. Mechanical Properties of PLLA/LG-g-PLMA Composites. The tensile strength of pure PLA was 55.6 MPa and the tensile strength decreased slightly after adding 1% or 3% LG-g-PLMA (Table 5). At 5% loading, the tensile strength decreased to 46.5 MPa. With further addition of 20% brought the tensile strength down to 26.5 MPa, a decrease of 52%. This phenomenon is due to the fact that the molecular structure of lignin determines its rigidity. With LMA grafting, a large number of flexible segments were introduced, and the molecular chain became flexible. When blended with PLA, flexible LG-g-PLMA will obviously reduce the tensile strength of PLA. Similar phenomena are also found in the work of Boarino,[49] Yang,[50] and others, and the more the addition, the greater the decline.

Table 5. Mechanical Properties of PLLA and PLLA/LG-g-PLMA Composites

sample	tensile strength (MPa)	strain at break (%)	elastic modulus (MPa)	toughness (MJ/m^3)
PLLA	55.6 ± 2.8	5.7 ± 0.4	938.8 ± 82.8	179.8 ± 5.2
PLLA1	55.2 ± 4.2	6.7 ± 0.8	647.8 ± 32.7	198.8 ± 4.2
PLLA2	50.8 ± 2.5	7.4 ± 0.3	598.9 ± 26.7	236.8 ± 5.6
PLLA3	46.5 ± 3.2	8.1 ± 1.3	744.8 ± 20.5	245.6 ± 12.3
PLLA4	41.8 ± 2.6	7.2 ± 0.8	652.2 ± 43.9	224.3 ± 5.5
PLLA5	40.8 ± 3.3	7.1 ± 0.6	869.1 ± 25.1	195.5 ± 4.8
PLLA6	26.5 ± 3.1	5.1 ± 0.2	559.2 ± 26.5	103.9 ± 3.6

The elongation at break showed just the opposite dependence of the tensile strength. Pure PLA had a low elongation at break of 5.7%, which increased to 6.7% at 1% loading of the graft copolymer. With the addition of 5% LG-g-PLMA, the maximal elongation at break was 8.1%. At higher loadings, i.e., when 7% or 9% LG-g-PLMA was added, the elongation at break declined slightly to 13% but was still higher than that of pure PLA. With further addition of LG-g-PLMA, the elongation at break continued to drop down to 5.1%. The main reason for the reversed V type change in elongation at break lied in the compatibility of the copolymer and PLA. After the introduction of LMA, LMA replaced part of the hydroxyl sites in LG, LMA brought hydrophobicity and flexibility to LG, improved the compatibility with PLA and thus enhanced the interfacial interaction between them. Therefore, a small amount of LG-g-PLMA can be evenly distributed in the PLA matrix. When the composite is subjected to tension, due to the strong interfacial adhesion, the external force can be effectively transferred from the PLA matrix to the flexible skeleton of the copolymer and the flexible skeleton would deform and absorb energy in the tensile direction, enhancing the toughness of the composite. When the external force exceeds the load-bearing limit of the flexible skeleton, the material will fracture. However, too high a loading would deteriorate and destroy the compatibility of the two and weaken the interface effect. Therefore, the transfer ability of external force will be reduced, and the fracture will occur in advance, leading to the change tendency mentioned above.[27,49,51]

In sharp contrast to LG-g-PLMA, the presence of 5% unmodified lignin reduced all mechanical properties of PLA. The tensile strength and elongation at break of the composites decreased to 33.2 MPa and 2.6%, respectively (Figure S5 and Table S4). This phenomenon indirectly proved that the introduction of LG-g-PLMA greatly improved the interfacial adhesion and the compatibility with PLA (Figure 10).

3.7. Micromorphological Analysis of PLLA/LG-g-PLMA Composites. SEM was used to observe the cryo-fractured surface morphology of PLLA/LG-g-PLMA mixtures with different compositions. It can be seen from Figure 11a that the surface of pure PLLA is relatively smooth, which is consistent with the characteristics of PLLA as a typical brittle material. With the addition of LG-g-PLMA, the island structure appeared in the blends, and the LG-g-PLMA particles were uniformly distributed in the PLA matrix. Compared with the smooth PLA surface, the roughness increased, indicating an enhancement in the interfacial adhesion between them. At 3% LG-g-PLMA addition, the wire drawing phenomenon (red circles) was observed, indicating that the cross section of the blend tends to change from brittleness to toughness. At a higher loading of 5%, a large number of pullout phenomena (green circles) and even local plastic deformation can be clearly seen, as shown in Figure 11d. This observation indicated that the composite exhibited has excellent toughness under this level of addition, which corresponds to its highest elongation at break. With the continuous addition of LG-g-PLMA, the size of distribution in the PLA matrix increased obviously, and a large number of surface protuberances and voids appeared. This phenomenon showed that the compatibility between LG-g-PLMA and the PLA matrix decreases, resulting in the aggregation of particles in the PLA matrix and the decrease of mechanical properties.

3.8. Optical Property of PLLA/LG-g-PLMA Composites. PLA is widely used as a packaging material, but its poor UV-blocking function limits its applications.[52] PLA readily undergoes oxidative degradation when exposed to UV light. Therefore, it is necessary to improve the UV barrier performance of PLA. Lignin has a strong blocking effect on UV radiation due to the existence of phenolic hydroxyl and

https://doi.org/10.1021/acsomega.3c01738
ACS Omega 2023, 8, 26926−26937

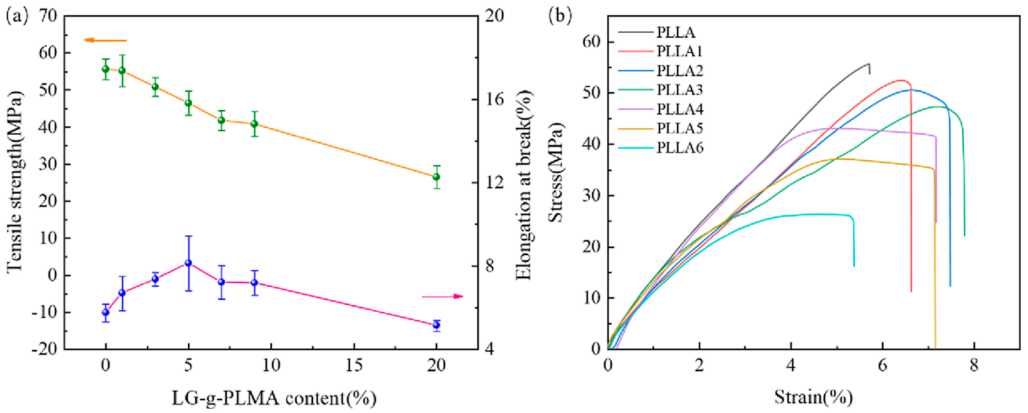

Figure 10. (a) Tensile strength and elongation at break of PLLA and PLLA/LG-g-PLMA composites. (b) Typical stress−strain curves of PLLA and PLLA/LG-g-PLMA composites.

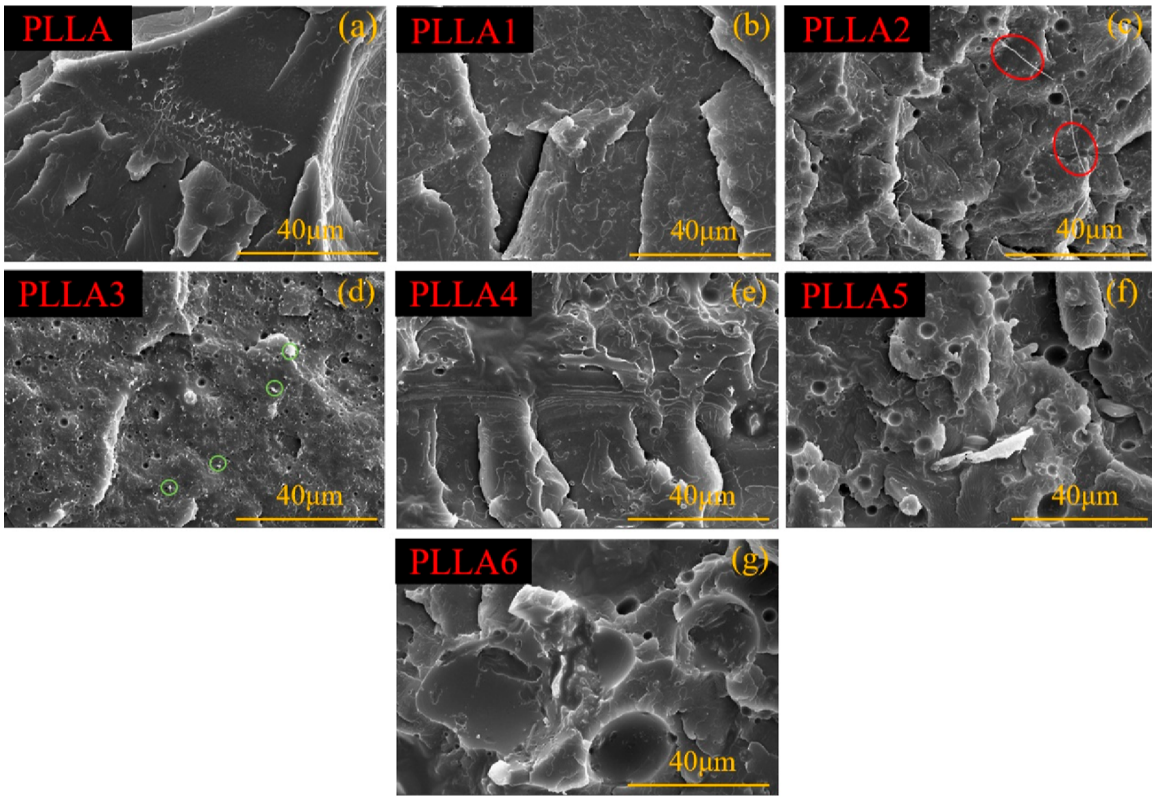

Figure 11. SEM images for the cryo-fractured surfaces of PLLA (a), PLLA1 (b), PLLA2 (c), PLLA3 (d), PLLA4 (e), PLLA5 (f), and PLLA6 (g).

methoxy groups.[30,45] The UV barrier properties of the composites can be improved by adding lignin. In addition, the grafted polymers are hydrophobic and expected to enhance the interface adhesion between lignin and PLA.[30,36] Thus, PLLA/LG-g-PLMA composites were expected to have significant UV barrier properties. Figure 12 shows that pure PLA had high transparency, with absorption only in the 200−250 nm region. It can be considered that pure PLA basically has no UV barrier properties. The addition of LG-g-PLMA obviously improved the UV barrier effect of composites. At 1% LG-g-PLMA addition, the transmittance in the 280−400 nm region is less than 30%, indicating that the composite can block most of the UV light. With further addition of LG-g-PLMA, it is obvious that the composite can almost completely block UV light; the transmittance in the 280−400 nm region is less than 1%. This superior UV barrier properties may be related to the increase of the proportion of lignin in the composites and its uniform dispersion in PLA.[37] Therefore, PLLA/LG-g-PLMA composites have potential application value in UV barrier packaging applications.

4. CONCLUSIONS

In this work, LMA was grafted onto lignin by convenient free-radical polymerization. Due to the long hydrophobic side chain in dodecyl methacrylate, the graft copolymer has better hydrophobicity and thermal stability. A wholly bio-based composite was prepared by blending LG-g-PLMA with PLA. It was found that the copolymer and PLA had excellent compatibility and strong interfacial adhesion. The mechanical properties of the composites are strengthened. At 5% loading, the composite has an elongation at break of 42%, higher than

https://doi.org/10.1021/acsomega.3c01738
ACS Omega 2023, 8, 26926−26937

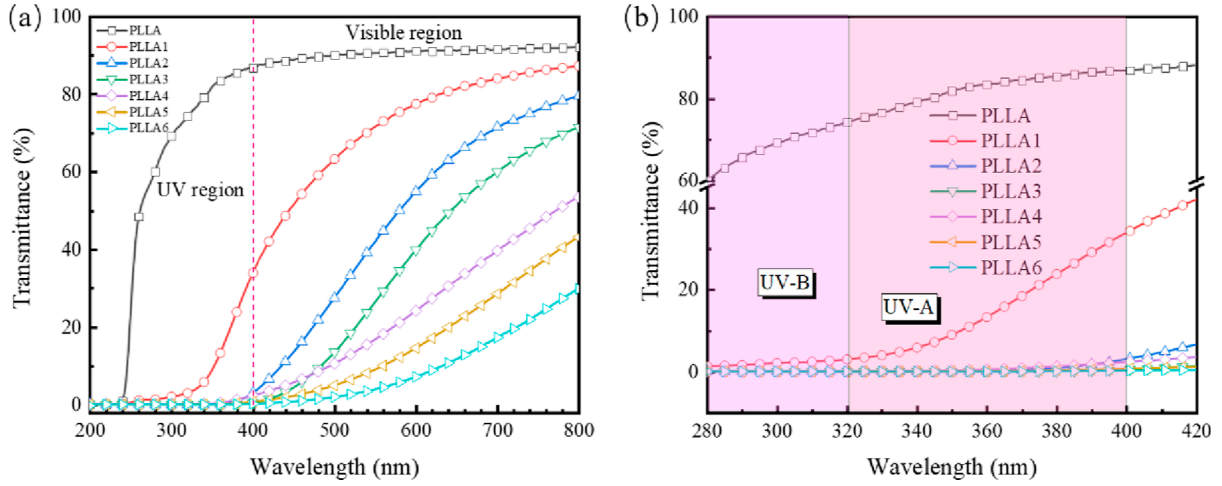

Figure 12. (a) UV−vis transmittance spectra for PLLA and PLLA/LG-g-PLMA composites. (b) 280−420 nm of UV−vis transmittance spectra.

that of PLA. Furthermore, it has a very strong UV barrier effect at a lower loading, almost completely blocking UV light. This work opens up a new way for the high-value utilization of lignin and provides a new idea for preparing all bio-based packaging materials for UV barriers.

■ ASSOCIATED CONTENT

Supporting Information

The Supporting Information is available free of charge at https://pubs.acs.org/doi/10.1021/acsomega.3c01738.

FT-IR spectra of LG, LG-g-PLMA, and LMA; DSC curves of PLLA7 composites; DSC curves of PLLA, PLLA7, and PLLA3 composites; non-isothermal crystallization parameters of PLLA, PLLA7, and PLLA3; TGA and DTG curves of PLLA7 composites; thermal property parameters of PLLA7 composites; TGA and DTG curves of PLLA, PLLA7, and PLLA3 composites; thermal property parameters of PLLA, PLLA7, and PLLA3 composites; and tensile strength and elongation at break of PLLA, PLLA7, and PLLA3 composites (PDF)

■ AUTHOR INFORMATION

Corresponding Authors

Hui Sun − *College of Chemistry and Materials Engineering, Beijing Technology and Business University, Beijing 100048, China; Beijing Key Laboratory of Quality Evaluation Technology for Hygiene and Safety of Plastics, Beijing Technology and Business University, Beijing 100048, China*; Email: sunhui@th.btbu.edu.cn

Yunxuan Weng − *College of Chemistry and Materials Engineering, Beijing Technology and Business University, Beijing 100048, China; Beijing Key Laboratory of Quality Evaluation Technology for Hygiene and Safety of Plastics, Beijing Technology and Business University, Beijing 100048, China*; Email: wyxuan@th.btbu.edu.cn

Authors

Kang Shi − *College of Chemistry and Materials Engineering, Beijing Technology and Business University, Beijing 100048, China*; orcid.org/0009-0006-1374-4051

Guoshuai Liu − *College of Chemistry and Materials Engineering, Beijing Technology and Business University, Beijing 100048, China*

Biao Yang − *College of Chemistry and Materials Engineering, Beijing Technology and Business University, Beijing 100048, China*

Complete contact information is available at: https://pubs.acs.org/10.1021/acsomega.3c01738

Notes

The authors declare no competing financial interest.

■ ACKNOWLEDGMENTS

Financial support from the National Natural Science Foundation of China (grant numbers: 31570575 and 52073004) was gratefully acknowledged.

■ REFERENCES

(1) Kuang, B.; Ning, M.; Wang, L.; Li, J.; Wang, C.; Hou, Z.; Zhao, Y.; Jin, H. Biopolymer nanofiber/reduced graphene oxide aerogels for tunable and broadband high-performance microwave absorption. *Composites, Part B* **2019**, *161*, 1−9.

(2) Ran, S.; Fang, F.; Guo, Z.; Song, P.; Cai, Y.; Fang, Z.; Wang, H. Synthesis of decorated graphene with P, N-containing compounds and its flame retardancy and smoke suppression effects on polylactic acid. *Composites, Part B* **2019**, *170*, 41−50.

(3) Kim, Y.; Kim, J. S.; Lee, S.-Y.; Mahajan, R. L.; Kim, Y.-T. Exploration of hybrid nanocarbon composite with polylactic acid for packaging applications. *Int. J. Biol. Macromol.* **2020**, *144*, 135−142.

(4) Li, R.; Wu, L.; Li, B.-G. Poly(L-lactide) Materials with Balanced Mechanical Properties Prepared by Blending with PEG-mb-PPA Multiblock Copolymers. *Ind. Eng. Chem. Res.* **2017**, *56*, 2773−2782.

(5) Ma, H.; Shen, J.; Yang, Q.; Zhou, J.; Xia, S.; Cao, J. Effect of the Introduction of Fish Collagen on the Thermal and Mechanical Properties of Poly(lactic acid). *Ind. Eng. Chem. Res.* **2015**, *54*, 10945−10951.

(6) Harynska, A.; Janik, H.; Sienkiewicz, M.; Mikolaszek, B.; Kucinska-Lipka, J. PLA-Potato Thermoplastic Starch Filament as a Sustainable Alternative to the Conventional PLA Filament: Processing, Characterization, and FFF 3D Printing. *ACS Sustainable Chem. Eng.* **2021**, *9*, 6923−6938.

(7) Ilyas, R. A.; Sapuan, S. M.; Harussani, M. M.; Hakimi, M. Y. A. Y.; Haziq, M. Z. M.; Atikah, M. S. N.; Asyraf, M. R. M.; Ishak, M. R.; Razman, M. R.; Nurazzi, N. M.; Norrrahim, M. N. F.; Abral, H.; Asrofi, M. Polylactic Acid (PLA) biocomposite: processing, additive manufacturing and advanced applications. *Polymers* **2021**, *13*, 1326.

(8) Jiang, X.; Li, Q.; Li, X.; Meng, Y.; Ling, Z.; Ji, Z.; Chen, F. Preparation and Characterization of Degradable Cellulose-Based Paper with Superhydrophobic, Antibacterial, and Barrier Properties for Food Packaging. *Int. J. Mol. Sci.* **2022**, *23*, 11158.
(9) Roy Goswami, S.; Sudhakaran Nair, S.; Zhang, X.; Tanguy, N.; Yan, N. Starch Maleate/Epoxidized Soybean Oil/Polylactic Acid Films with Improved Ductility and Biodegradation Potential for Packaging Fatty Foods. *ACS Sustainable Chem. Eng.* **2022**, *10*, 14185−14194.
(10) Lasprilla, A. J. R.; Martinez, G. A. R.; Lunelli, B. H.; Jardini, A. L.; Filho, R. M. Poly-lactic acid synthesis for application in biomedical devices - A review. *Biotechnol. Adv.* **2012**, *30*, 321−328.
(11) Valente, T. A. M.; Silva, D. M.; Gomes, P. S.; Fernandes, M. H.; Santos, J. D.; Sencadas, V. Effect of Sterilization Methods on Electrospun Poly(lactic acid) (PLA) Fiber Alignment for Biomedical Applications. *ACS Appl. Mater. Interfaces* **2016**, *8*, 3241−3249.
(12) Zhang, S.; Li, H.; Yuan, M.; Yuan, M.; Chen, H. Poly(lactic acid) blends with poly(trimethylene carbonate) as biodegradable medical adhesive material. *Int. J. Mol. Sci.* **2017**, *18*, 2041.
(13) Hollingshead, S.; Siebert, H.; Wilker, J. J.; Liu, J. C. Cytocompatibility of a mussel-inspired poly(lactic acid)-based adhesive. *J. Biomed. Mater. Res., Part A* **2022**, *110*, 43−51.
(14) Jiang, L.; Wolcott, M. P.; Zhang, J. Study of biodegradable polylactide/poly(butylene adipate-co-terephthalate) blends. *Biomacromolecules* **2006**, *7*, 199−207.
(15) Balakrishnan, H.; Hassan, A.; Imran, M.; Wahit, M. U. Toughening of Polylactic Acid Nanocomposites: A Short Review. *Polym.-Plast. Technol. Eng.* **2012**, *51*, 175−192.
(16) Zolali, A. M.; Favis, B. D. Toughening of Cocontinuous Polylactide/Polyethylene Blends via an Interfacially Percolated Intermediate Phase. *Macromolecules* **2018**, *51*, 3572−3581.
(17) Zhang, T.; Han, W.; Zhang, C.; Weng, Y. Effect of chain extender and light stabilizer on the weathering resistance of PBAT/PLA blend films prepared by extrusion blowing. *Polym. Degrad. Stab.* **2021**, *183*, 109455.
(18) Gu, L.; Macosko, C. W. Evaluating PE/PLA interfacial tension using ternary immiscible polymer blends. *J. Appl. Polym. Sci.* **2021**, *138*, 50623.
(19) Garlapati, V. K.; Chandel, A. K.; Kumar, S. J.; Sharma, S.; Sevda, S.; Ingle, A. P.; Pant, D. Circular economy aspects of lignin: Towards a lignocellulose biorefinery. *Renew. Sustain. Energy Rev.* **2020**, *130*, 109977.
(20) Constant, S.; Wienk, H. L. J.; Frissen, A. E.; Peinder, P. d.; Boelens, R.; van Es, D. S.; Grisel, R. J. H.; Weckhuysen, B. M.; Huijgen, W. J. J.; Gosselink, R. J. A.; Bruijnincx, P. C. A. New insights into the structure and composition of technical lignins: a comparative characterisation study. *Green Chem.* **2016**, *18*, 2651−2665.
(21) Figueiredo, P.; Lintinen, K.; Hirvonen, J. T.; Kostiainen, M. A.; Santos, H. A. Properties and chemical modifications of lignin: Towards lignin-based nanomaterials for biomedical applications. *Prog. Mater. Sci.* **2018**, *93*, 233−269.
(22) Hambardzumyan, A.; Foulon, L.; Chabbert, B.; Aguie-Beghin, V. Natural Organic UV-Absorbent Coatings Based on Cellulose and Lignin: Designed Effects on Spectroscopic Properties. *Biomacromolecules* **2012**, *13*, 4081−4088.
(23) Ko, H.-U.; Kim, J. W.; Kim, H. C.; Zhai, L.; Kim, J. Esterified PVA-lignin resin by maleic acid applicable for natural fiber reinforced composites. *J. Appl. Polym. Sci.* **2020**, *137*, 48836.
(24) Zheng, Q.; Xie, H.; He, Y.; Sun, H.; Chen, X.; Guo, J.; Wang, J.; He, Y.; Chen, X.; Zheng, Q.; Sun, H.; Chen, X.; Zheng, Q. Triply Biobased Thermoplastic Composites of Polylactide/Succinylated Lignin/Epoxidized Soybean Oil. *Polymers* **2020**, *12*, 632.
(25) Xiong, S.-J.; Pang, B.; Zhou, S.-J.; Li, M.-K.; Yang, S.; Wang, Y.-Y.; Shi, Q.; Wang, S.-F.; Yuan, T.-Q.; Sun, R.-C. Economically Competitive Biodegradable PBAT/Lignin Composites: Effect of Lignin Methylation and Compatibilizer. *ACS Sustainable Chem. Eng.* **2020**, *8*, 5338−5346.
(26) Liu, H.; Chung, H. Lignin-based Polymers via Graft Copolymerization. *J. Polym. Sci., Part A: Polym. Chem.* **2017**, *55*, 3515.
(27) Sun, Y.; Ma, Z.; Xu, X.; Liu, X.; Liu, L.; Huang, G.; Liu, L.; Wang, H.; Song, P. Grafting Lignin with Bioderived Polyacrylates for Low-Cost, Ductile, and Fully Biobased Poly(lactic acid) Composites. *ACS Sustainable Chem. Eng.* **2020**, *8*, 2267−2276.
(28) Zong, E.; Liu, X.; Liu, L.; Wang, J.; Song, P.; Ma, Z.; Ding, J.; Fu, S. Graft Polymerization of Acrylic Monomers onto Lignin with CaCl2-H2O2 as Initiator: Preparation, Mechanism, Characterization, and Application in Poly(lactic acid). *ACS Sustainable Chem. Eng.* **2018**, *6*, 337−348.
(29) Muiruri, J. K.; Liu, S.; Teo, W. S.; Kong, J.; He, C. Highly Biodegradable and Tough Polylactic Acid-Cellulose Nanocrystal Composite. *ACS Sustainable Chem. Eng.* **2017**, *5*, 3929−3937.
(30) Chung, Y.-L.; Olsson, J. V.; Li, R. J.; Frank, C. W.; Waymouth, R. M.; Billington, S. L.; Sattely, E. S. A Renewable Lignin-Lactide Copolymer and Application in Biobased Composites. *ACS Sustainable Chem. Eng.* **2013**, *1*, 1231−1238.
(31) Huang, W.; Wu, M.; Liu, W.; Hua, Z.; Wang, Z.; Zhou, L. Value-adding of organosolv lignin: Designing mechanically robust UV-resistant polymeric glass via ARGET ATRP. *Appl. Surf. Sci.* **2019**, *475*, 302−311.
(32) Wu, M.; Wu, M.; Pan, M.; Jiang, F.; Hui, B.; Zhou, L. Synthesization and Characterization of Lignin-graft-Poly (Lauryl Methacrylate) via ARGET ATRP. *Int. J. Biol. Macromol.* **2022**, *207*, 522−530.
(33) Kong, F. G.; Wang, S. J.; T Price, J.; Konduri, M. K. R.; Fatehi, P. Water soluble kraft lignin-acrylic acid copolymer: synthesis and characterization. *Green Chem.* **2015**, *17*, 4355−4366.
(34) Zhang, Z.; Mulyadi, A.; Kuang, X.; Liu, W.; Li, V.; Gogoi, P.; Liu, X. L.; Deng, Y. L. Lignin-polystyrene composite foams through high internal phase emulsion polymerization. *Polym. Eng. Sci.* **2019**, *59*, 964−972.
(35) Panesar, S. S.; Jacob, S.; Misra, M.; Mohanty, A. K. Functionalization of lignin: Fundamental studies on aqueous graft copolymerization with vinyl acetate. *Ind. Crops Prod.* **2013**, *46*, 191−196.
(36) Liu, X.; Xu, Y.; Yu, J.; Li, S.; Wang, J.; Wang, C.; Chu, F. Integration of lignin and acrylic monomers towards grafted copolymers by free radical polymerization. *Int. J. Biol. Macromol.* **2014**, *67*, 483−489.
(37) Zhang, N.; Zhao, M.; Liu, G.; Wang, J.; Chen, Y.; Zhang, Z. Alkylated lignin with graft copolymerization for enhancing toughness of PLA. *J. Mater. Sci.* **2022**, *57*, 8687−8700.
(38) Maiti, B.; De, P. RAFT polymerization of fatty acid containing monomers: controlled synthesis of polymers from renewable resources. *RSC Adv.* **2013**, *3*, 24983−24990.
(39) Yu, J.; Lu, C.; Wang, C.; Wang, J.; Fan, Y.; Chu, F. Sustainable thermoplastic elastomers derived from cellulose, fatty acid and furfural via ATRP and click chemistry. *Carbohydr. Polym.* **2017**, *176*, 83−90.
(40) Cai, Y. H.; Yan, S. F.; Yin, J. B.; Fan, Y. Q.; Chen, X. S. Crystallization Behavior of Biodegradable Poly(L-lactic acid) Filled with a Powerful Nucleating Agent: N,N'-Bis(benzoyl) Suberic Acid Dihydrazide. *J. Appl. Polym. Sci.* **2011**, *121*, 1408−1416.
(41) Cheng, Y.; Lin, J.; Zheng, Y.; Chen, X.; Lu, C. High-Performance Gel-Spun Poly(vinyl alcohol) Fibers Reinforced by Organosolv Lignin-graft-poly(acrylic acid). *Ind. Eng. Chem. Res.* **2022**, *61*, 6037−6051.
(42) Cheng, Z.; Liu, Y.; Zhang, D.; Lu, C.; Wang, C.; Xu, F.; Wang, J.; Chu, F. Sustainable elastomers derived from cellulose, rosin and fatty acid by a combination of "graft from" RAFT and isocyanate chemistry. *Int. J. Biol. Macromol.* **2019**, *131*, 387−395.
(43) Liu, X.; Wang, J.; Li, S.; Zhuang, X.; Xu, Y.; Wang, C.; Chu, F. Preparation and properties of UV-absorbent lignin graft copolymer films from lignocellulosic butanol residue. *Ind. Crops Prod.* **2014**, *52*, 633−641.
(44) Jiang, F.; Wang, Z.; Qiao, Y.; Wang, Z.; Tang, C. A Novel Architecture toward Third-Generation Thermoplastic Elastomers by a Grafting Strategy. *Macromolecules* **2013**, *46*, 4772−4780.

https://doi.org/10.1021/acsomega.3c01738
ACS Omega 2023, 8, 26926−26937

(45) Ren, W.; Pan, X.; Wang, G.; Cheng, W.; Liu, Y. Dodecylated lignin-g-PLA for effective toughening of PLA. *Green Chem.* **2016**, *18*, 5008−5014.
(46) Liu, W.; Qiu, J.; Fei, M.-e.; Qiu, R.; Sakai, E. Manufacturing of Thermally Remoldable Blends from Epoxidized Soybean Oil and Poly(lactic acid) via Dynamic Cross-Linking in a Twin-Screw Extruder. *Ind. Eng. Chem. Res.* **2018**, *57*, 7516−7524.
(47) Zhang, J.; Tashiro, K.; Tsuji, H.; Domb, A. J. Disorder-to-Order Phase Transition and Multiple Melting Behavior of Poly(L-lactide) Investigated by Simultaneous Measurements of WAXD and DSC. *Macromolecules* **2008**, *41*, 1352−1357.
(48) Prieur, B.; Meub, M.; Wittemann, M.; Klein, R.; Bellayer, S.; Fontaine, G.; Bourbigot, S. Phosphorylation of lignin to flame retard acrylonitrile butadiene styrene (ABS). *Polym. Degrad. Stab.* **2016**, *127*, 32−43.
(49) Boarino, A.; Schreier, A.; Leterrier, Y.; Klok, H.-A. Uniformly Dispersed Poly(lactic acid)-Grafted Lignin Nanoparticles Enhance Antioxidant Activity and UV-Barrier Properties of Poly(lactic acid) Packaging Films. *ACS Appl. Polym. Mater.* **2022**, *4*, 4808−4817.
(50) Yang, W.; Zhu, Y.; He, Y.; Xiao, L.; Xu, P.; Puglia, D.; Ma, P. Preparation of toughened poly(lactic acid)-poly(ε-caprolactone)-lignin nanocomposites with good heat- and UV-resistance. *Ind. Crops Prod.* **2022**, *183*, 114965.
(51) Sun, Y.; Yang, L.; Lu, X.; He, C. Biodegradable and renewable poly(lactide)-lignin composites: synthesis, interface and toughening mechanism. *J. Mater. Chem. A* **2015**, *3*, 3699−3709.
(52) Rasselet, D.; Ruellan, A.; Guinault, A.; Miquelard-Garnier, G.; Sollogoub, C.; Fayolle, B. Oxidative degradation of polylactide (PLA) and its effects on physical and mechanical properties. *Eur. Polym. J.* **2014**, *50*, 109−116.

https://doi.org/10.1021/acsomega.3c01738
ACS Omega 2023, 8, 26926−26937